Journal of African Earth Sciences 160 (2019) 103651

Contents lists available at ScienceDirect

Journal of African Earth Sciences

journal homepage: www.elsevier.com/locate/jafrearsci

Mineralogical and geochemical characterization of radioactive minerals and rare earth elements in granitic pegmatites at G. El Fereyid, South Eastern Desert, Egypt

G.M. Saleh[a], A.M. Afify[b,*], B.M. Emad[a], M.I. Dawoud[c], H.A. Shahin[a], F.M. Khaleal[a]

[a] Nuclear Materials Authority, El Maadi, Cairo, Egypt
[b] Department of Geology, Faculty of Science, Benha University, 13518, Benha, Egypt
[c] Geology Department, Faculty of Science, Menoufia University, Shebin El-Kom, Egypt

ARTICLE INFO

Keywords:
Mineralogy
Geochemistry
Rare earth elements
Radioactive minerals
Granitic pegmatites
Egypt

ABSTRACT

The present work deals with the mineralogical and geochemical investigations of radioactive minerals and rare earth elements associated with granitic pegmatites at Gabal El Fereyid area exposed in the south Eastern Desert of Egypt. The study area is occupied by tonalite and monzogranites, the latter is intruded by pegmatites with a distinctive distribution of economically important mineralization. The studied pegmatitic bodies occur as veins that are ranging in size from few meters to 25 m long and their width usually less than 7 m; although small pockets are present. The latter display zoning structure (concentric layering) consisting of feldspar-rich zones enveloping pockets of mica (mainly muscovite) and all zoning internal quartz core. Field work using gamma spectroscopy measurements over these pegmatites shows that some bodies are radiometrically anomalous, especially the muscovite-rich zones. The mineralogy and geochemistry (trace and rare earth elements contents) of the radioactive zones in such pegmatites were achieved.

Mineral characterization of the highly radioactive zones shows enrichment in thorite, uranothorite, ishikawaite, samarskite and fergusonite minerals. The spectrometric measurements of the studied pegmatites show that they possess the highest content of radioelements as well. They show enrichment in large ion lithophile elements (LILE; Pb, Rb, Sr) and high field strength elements (HFSE; Y, Zr, Th, U, Nb) and depletion in K, P and Ti. The studied granitic pegmatites indicate moderate to large negative Eu anomaly and show clear M-type tetrad effect of REE.

The mineralogical and geochemical signature of investigated pegmatites represents a NYF-type (Niobium–Yttrium–Fluorine family), whereas the enrichment of rare element is an indication of high degrees of fractional crystallization of a suite of volatile-rich magmas. Uranium and thorium mineralization in the studied pegmatite are related to magmatic (syngenetic) origin with hydrothermal (epigenetic) input. The magmatic mineralization is evidenced by occurrence of thorite and zircon, whereas the hydrothermal activity is represented by alteration of feldspars and formation of pyrite and iron oxides associated with the radioactive minerals.

The high levels of radioactivity and rare earth elements mineralization in the studied granitic pegmatite bodies make them a target to exploration and to enlarge the potentiality of the highly mineralized localities.

1. Introduction

Granitic pegmatites are reliable sources of radioactive minerals and rare earth elements worldwide where they show enrichment in Li, Cs, Be, Nb, Ta, Sn, Zr, Hf, U, Th, Mo, REE, and other economic elements (Černý, 1990, 1991; El Aassy et al., 1997; Salem et al., 1998; Heikal et al., 2001; Černý et al., 2012). In the last years, uses of these rare earth elements and radioactive minerals expanded rapidly either for production of high technology, commercial, industrial production and/or for energy. Accordingly, study of granitic pegmatites and their associated economic minerals attracted the attention of mineralogists in the last decades and it is expected that the demand for such elements will grow in the future. Many promising characteristics, e.g., distribution, rock compositions, mineralogy and isotopic characteristics, reveals

* Corresponding author.
E-mail addresses: adel_geol@yahoo.com, adel.mohamed@fsc.bu.edu.eg (A.M. Afify).

https://doi.org/10.1016/j.jafrearsci.2019.103651
Received 6 May 2019; Received in revised form 7 September 2019; Accepted 23 September 2019
Available online 24 September 2019
1464-343X/

genetic relationship between granites and the intruding pegmatites (Walker, 1984; Thomas and Webster, 2000). As well, the granitic pegmatites are well-known for the diversity and concentrations of metalliferous ores and rare elements they host.

Distribution and occurrence of radioactive minerals in Egypt are dominant mostly in younger granites and their associated pegmatites (Abdel-Karim, 1999; Abd El Naby and Saleh, 2003). The host granites are post-orogenic to anorogenic, which themselves constitute a target for rare earth elements and exploration in Egypt. Radioactive granitic pegmatites were reported in many areas of the Egyptian Eastern Desert (e.g., Wadi Zareib, Red Ashab, Dahab, G. Um Anab, G. Ras Baroud, G. El Sibai, G. Abu Dob (Sayyah et al., 1993; Omar, 1995; Ibrahim et al., 1997; Salem et al., 1998; Ibrahim et al., 2001; Ali, 2001; Heikal et al., 2001; Raslan et al., 2010)). Peculiar pegmatites associated with the granitic rocks were reported, as well, in the southern part of the Eastern Desert; e.g., G. Ribdab (Ibrahim et al., 2001), G. El Fereyid (Abd El Naby and Saleh, 2003). Rare-element pegmatites, together with numerous outcrops of younger granites, are common in the Precambrian basement complex especially the northern domain of the Eastern Desert: e.g., Wadi Dara, Gabal Abu Khashaba, Wadi Hawashia and Gabal El Urf (Shalaby, 1985; Nossair, 1987; Mohamed et al., 1994; Ali, 2007; Asran et al., 2013).

The geology, structure, mineralogy and geochemistry of the present area was studied by Soliman et al. (1985a, b), El-Eraqi (1990), El Amawy (1991), El-Baraga (1992), Abdel Karim and Sos (2000), Abd El-Naby and Saleh (2003), Saleh et al. (2018) and Dawoud et al. (2018). Even though, the mineralization of rare earth elements and radioactive minerals in the granitic pegmatites were not achieved. Accordingly, the present work will shed the light on the mineralization, spectrometric prospecting and geochemical attributes of radioactive and rare earth elements associated with the granitic pegmatites at Gabal El Fereyid area in the south Eastern Desert of Egypt.

2. Geologic setting

The study area is located between latitudes 23° 15′- 23° 19′ N and longitudes 35° 22′ - 35° 22′ E in south Eastern Desert (Fig. 1). The field study along with the structural observations and petrography of the basement rocks encountered in the area revealed tonalites, monzogranite and pegmatites from older to younger respectively according to their stratigraphic position (Saleh et al., 2018) (Fig. 1). The tonalite rocks occur as grey, highly exfoliated low hills which are invaded by biotite monzogranite and biotite leucogranite (Fig. 2a) and basic dykes (Fig. 2b). The monzogranite rocks form the main granitic masses that are elongated usually in NW-SE directions (Fig. 1). They are reddish grey, medium to coarse-grained, jointed, massive, exfoliated and highly sheared and leucocratic (Saleh et al., 2018). The monzogranites are intruded by dominant fine-grained granitic dykes (acidic dykes) (Fig. 2c) and quartz veins (Fig. 2d). The basic and acidic dykes intruding the monzogranite rocks attitude a NE-SW direction (Fig. 1).

The monzogranites are hosted by granitic pegmatites which occur as veins, pockets and/or rarely as dykes (Fig. 2e, f, g). These granitic pegmatites are randomly distributed as irregular bodies in the northwestern and southern parts of the study area (Fig. 1). They are very coarse grained, reddish to buff, whitish to grayish black colors. The vein-like pegmatites ranges in size from few meters to 25 m long and their width usually less than 7 m (Fig. 2e). Whereas the pocket-like bodies of the studied pegmatites display zoning structure with diameter approximately 50–70 cm and consisting of feldspar-rich zones

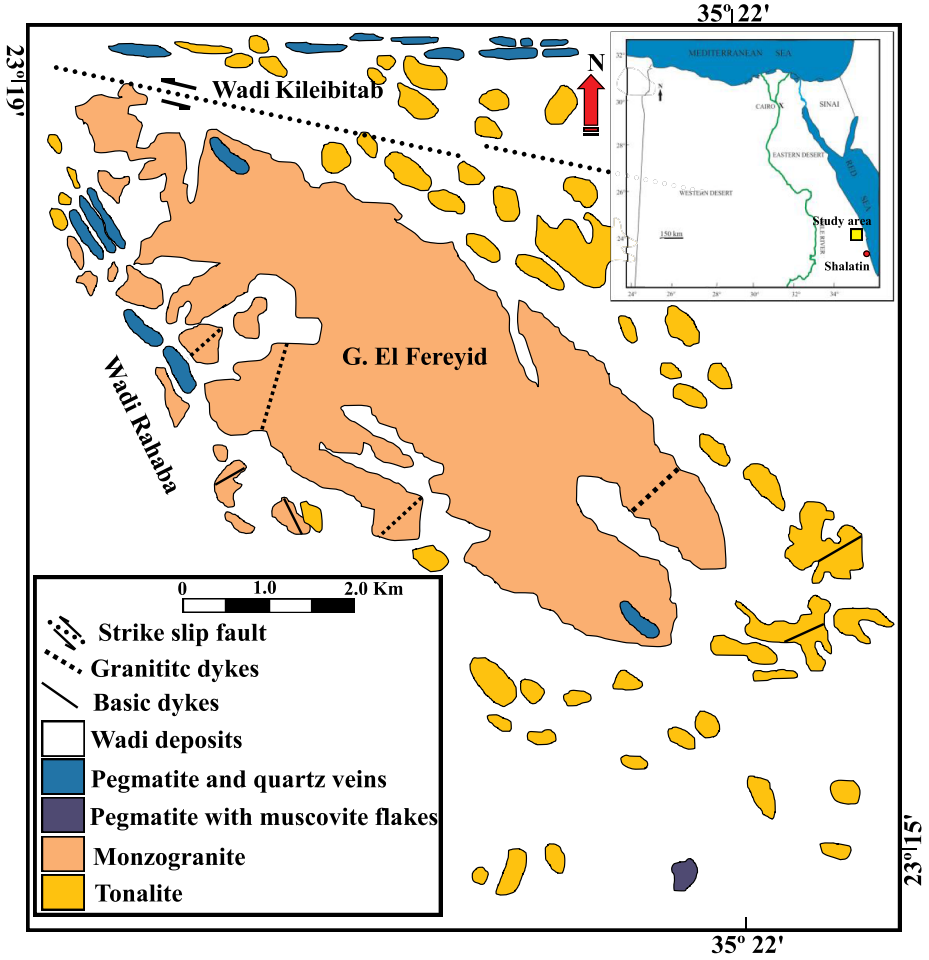

Fig. 1. A geologic map of G. El Fereyid area, South Eastern Desert, Egypt (after Abd El Naby and Saleh, 2003).

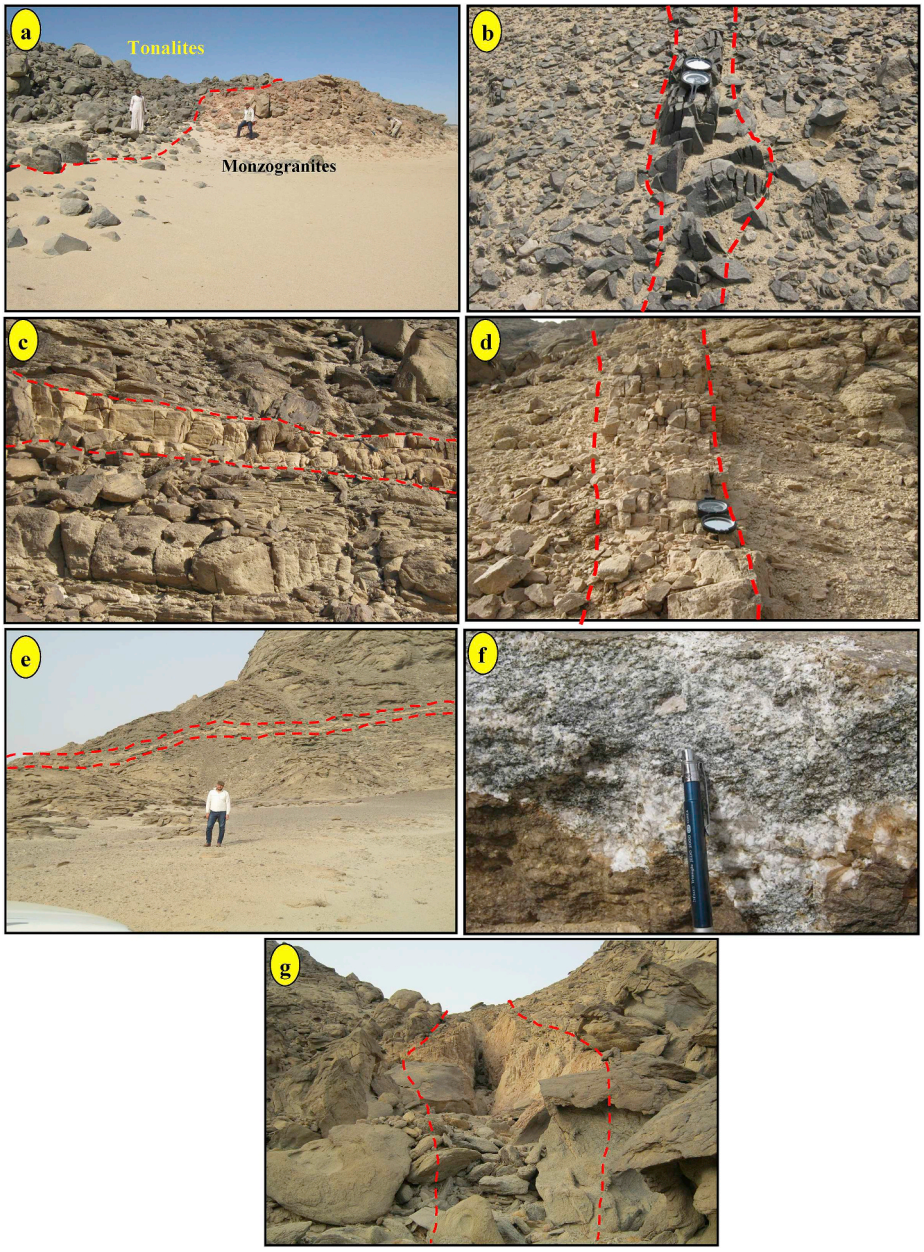

Fig. 2. Field photographs of G. El Fereyid area, SED, Egypt showing a) Contact between the intrusive monzogranites and tonalites. b) Basic dyke crosscut tonalites (Looking N–S), c) Granitic dyke intruding the monzogranite (Looking NE), d) Subvertical quartz vein cutting the monzogranites (Looking N–S), e) Quartz-rich pegmatite vein cutting the monzogranite (Looking N). f) Close-up view of muscovite-rich pegmatite intruded in the monzogranite, and g) Pegmatitic dyke cross-cutting the monzogranites.

enveloping pockets of mica (mainly muscovite; Fig. 2f) and all zoning internal quartz core. The dyke-like granitic pegmatites range in length from 100 to 200 m and width less than 8 m (Fig. 2g). More details about the granitic pegmatites are discussed below in the following chapters.

The study area is dominated by a heterogeneous brittle to ductile deformation. It was influenced by a major NW-SE strike-slip fault affecting the northern part of the mapped area (Fig. 1) (Saleh et al., 2018). The structural analysis shows presence of a prominent set of folds with axes striking WNW to NW and a less prominent set with pronounced ENE and NNW trends (El Amawy, 1991; Saleh et al., 2018).

3. Materials and methods

The field work was achieved by collection of more than fifty samples from the pegmatites and their host monzogranitic rocks. For microscopic investigations, twenty thin sections were prepared for the granitic pegmatites to identify their main rock forming minerals and their textures. Heavy minerals, especially rare metal-bearing phases were achieved from low-density minerals through a standard heavy liquid method, using bromoform, then washed and dried. The resulting magnetic and non-magnetic heavy mineral fractions were studied under a binocular microscope. SEM image and semi-quantitative analyses of the picked mineral grains were identified by a Phillips XL 30 Scanning Electron microscope at the laboratory of the Nuclear Materials Authority of Egypt. Thirteen granitic pegmatite samples were selected from the highly radioactive zones whereas seven samples from the monzogranites were used for geochemical comparison. Major oxides and trace elements were analyzed for these twenty samples using XRF (X-ray fluorescent spectroscopy), whilst rare earth elements were analyzed using ICP-MS (inductively coupled plasma – mass spectrometry) at the ACME Analytical Laboratory,

Vancouver, Canada. Ground gamma ray spectrometric survey measurements have been determined using RS-230 instrument. Such measurements are dose rate (D.R.) in mSvh-1, concentration of equivalent uranium (eU) in ppm, equivalent thorium (eTh) in ppm and potassium (K) in %. Uranium mobilization (eUm) for the studied pegmatites and their host monzogranite is calculated by the difference between the measured eU and the expected original uranium. The latter is calculated by dividing the measured eTh by the average of eTh/eU ratio in the acidic crustal rocks (original uranium = eTh/3.5) to give the leaching values of uranium (eUm = eU - eTh/3.5) (Cambon, 1994).

4. Results

4.1. Pegmatite – host rock interaction

The studied granitic pegmatites with their associated rare earth elements and radioactive minerals appear usually as irregular bodies, pockets, veins and/or dykes (Fig. 2e, f, g) hosted in the monzogranitic rocks. This represents a complete in-situ sequence from granitic to highly evolved pegmatites. The contact of the pegmatite bodies (veins, dykes, pockets) with the host monzogranites is sharp (Fig. 2e, f, g). On

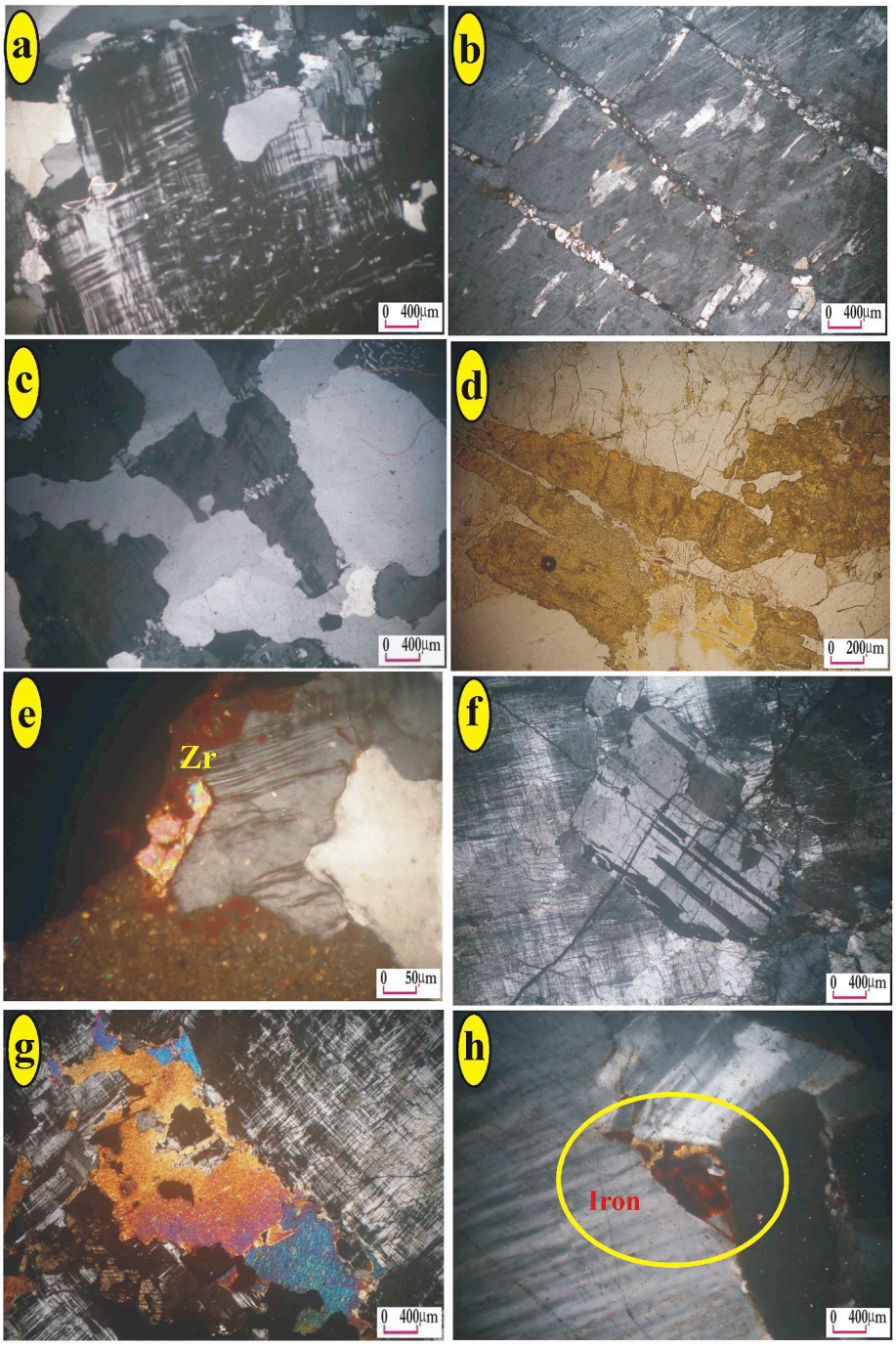

Fig. 3. Photomicrographs of granitic pegmatites of G. El Fereyid area clarifying a) Megacryst of microcline perthite, b) Megacryst of antiperthite dissected by fractures of secondary silica, c) Skeletal crystals of quartz included in megacrystal of microcline, d) Crystal of Fergusonite associated with quartz, e) Anhedral crystal of zircon (Zr) in crystal of plagioclase, f) Euhedral crystal of albite enclosed in megacryst of microcline and g) Megacryst of microcline enclosing flake of biotite and iron oxides, and h) Secondary iron oxide associated with amorphous radioactive minerals in string perthite. All photos are in crossed nichols except (d) in ppl.

basis of their mineralogy and morphology, the pegmatites are granitic in nature with dominance of feldspars (orthoclase and microcline), quartz and sometimes muscovite.

The granitic pegmatites are rich in quartz and K-feldspars which are dominant in the northern and northwestern parts of the study area (Fig. 1), cutting across the monzogranite with a NW-SE strike and with variable dips (Fig. 2d). The granitic pegmatites with dominance of muscovite are very coarse-grained and contain large individual crystals of their constituents (Fig. 2f) and found as irregular bodies distributed in the southern part of the area (Fig. 1). From the in-situ gamma-ray spectrometric surveys (described below), the highest radioelement concentrations were determined in the granitic pegmatite samples rich in muscovite if compared with the granitic pegmatite poor in muscovite.

4.2. Petrography

Microscopically, the studied pegmatites hosted within the monzogranite are composed essentially of potash feldspar, quartz, plagioclase, and mafic minerals (biotite, hornblende) with grains reached up to 2 cm (Fig. 3). Potash feldspar occurs as euhedral to subhedral mega-crystals represented mainly by microcline perthite and antiperthite (Fig. 3a and b). Perthite crystals are strained and characterized by fracturing, undulose extinction. They are dissected by fractures of secondary quartz (silicification process). Plagioclase is a minor constituent occurring as fine crystals included in the megacrysts of potash feldspar. It shows pericline-albite twinning and mainly altered to sericite, with quartz crystals showing myrmeckitic texture. Quartz occurs as skeletal crystals digested by the mega-crystals of microcline and exhibiting wavy extinction (Fig. 3c). Biotite occurs as irregular flakes associated with plagioclase filling fractures in the potash feldspar or found as elongated flakes aligned along the fracture in quartz. Fergusonite is the main accessory mineral occurring as euhedral prismatic crystals with its pale brown color included in the mega-crysts of quartz (Fig. 3d). It is completely isotropic attributed to metamictization due to its radioactive signatures. Zircon present as fractured crystals, mostly due to compression, coated by iron oxides and associating plagioclase crystals (Fig. 3e). Some of the fractures in the microcline mega-crysts filled by albite, biotite flakes and iron oxides which may be accompanied by amorphous radioactive minerals (Fig. 3f, g and h).

4.3. Mineralogy and high-resolution grain analysis of the granitic pegmatites

A combination of binocular microscope, scanning electron microscope (SEM/EDX) and back-scattered electron imaging (BSE) analysis of heavy minerals associated with the studied granitic pegmatites revealed the dominance of thorite ($ThSiO_4$), uranothorite ((Th, U) SiO_4), monazite ((Ce, La, Nd, Th) PO_4), zircon ($ZrSiO_4$), fergusonite (Nb, Y, Ta, U, Al, Mg, Fe, REE), samarskite ((Y, Ce, U, Fe)$_3$ (Nb, Ta, Ti)$_5O_{16}$), ishikawaite ((U, Fe, Ca, Y, Th) (Nb, Ta, Ti)$_2$ O_6) with subordinate amount of pyrite (FeS_2), titanite ($CaTiSiO_5$), allanite ((Ca, Ce, La)$_2$ (Al, Fe^{3+}, Fe^{2+})$_3O$. SiO_4. Si_2O_7. OH) and fluorite (CaF_2) minerals. Crystal morphologies, occurrences, description and semi-quantitative analysis of these minerals using SEM/EDX are shown in Table 1 and Fig. 4.

4.4. Geochemistry of the granitic pegmatites and their host rocks

Representative chemical analyses of thirteen mineralized pegmatite samples and seven samples of the host monzogranites are listed in Tables 2 and 3. Geochemistry of major, trace and rare earth elements of these granitic pegmatites and their host monzogranites are described as follows.

4.4.1. Major and trace element geochemistry

The major element compositions of the investigated pegmatites reveal the granitic nature of these rocks and their advanced degree of magmatic evolution. Compared to the average of El Fereyid monzogranites (seven samples for comparison), the pegmatite samples have high contents of silica (av. 75.55 wt%), total iron (4.41 wt%), CaO (av. 0.18 wt%) and Na_2O (av. 4.25 wt%). The other oxides are relatively constant with TiO_2 (av. 0.15%), Al_2O_3 (av. 13.55 wt%), MnO (av. 0.06 wt%), MgO (av. 0.13 wt%), K_2O (av. 4.25 wt%) and P_2O_5 (av. 0.02 wt%) (Tables 2 and 3).

The Na_2O content of pegmatite samples is plotted versus to K/Cs ratio (Fig. 5a), where the boundaries between the mica and rare-element (Cs- and Li-bearing) pegmatites are shown (Gordiyenko, 1971; Trueman and Černý, 1982). Composition points of potash-feldspar from the El Fereyid pegmatites are found predominantly in Li-bearing pegmatite field from Canada (Trueman and Černý, 1982).

Barium content of pegmatite samples is plotted versus to K/Rb ratio (Fig. 5b) where they show a positive relationship. The Li content is plotted against the K/Rb ratio for the studied pegmatites (Fig. 5c) where they fall in rare-elements class field according to Černý and Burt (1984) diagram.

The Nb/Ta ratios for the pegmatite samples have average 8.7 ppm, that is lower than the average ratio of El Fereyid monzogranite (13.2 ppm). The average Zr/Hf ratio is 24.3 for all pegmatite samples, which is lower than the average (31.5 ppm) of El Fereyid monzogranites. There is an increase in Hf, with relatively constant Zr/Hf ratios. In pegmatite samples, Hf is enriched with respect to Zr in the zircons.

The average of trace element concentrations of pegmatite samples is

Table 1
Summary of the mineralogy of radioactive minerals studied in the pegmatites of G. El Fereyid at the South Eastern Desert of Egypt. Crystal morphologies and description of these minerals are described as well.

Mineral	Chemical composition	Crystal morphologies and Description	SEM/EDX analysis
Thorite	($ThSiO_4$)	Small shiny dark red crystals mostly associated with iron oxides.	70.30 wt% Th, 10.13 wt% U, 3.90 wt% Fe, 2.97 wt% Al and 10.00 wt% Si (Fig. 4a).
Uranothorite	((Th, U) SiO_4)	Yellowish red crystals vitreous to sub-resinous crystals that are mostly associated with zircon (Fig. 4b).	59.79 wt% Th, 15.16 wt% U, 19.04 wt% Zr, 3.01 wt% Fe, 1.97 wt% Al and 16.84 wt% Si (Fig. 4b).
Monazite	((Ce, La, Nd, Th) PO_4)	Yellow, brown to red colors with resinous luster (Fig. 4c).	42.03 wt% Y, 42.33 wt% P, 2.44 wt% Gd, 3.40 wt% Dy, 2.19 wt% La, 5.76 wt% Th and 2.11 wt% U (Fig. 4c).
Zircon	($ZrSiO_4$)	Prismatic with bipyramidal faces and some are with sub-rounded edges (Fig. 4d).	30.99 wt% Zr, 62.93 wt% Si, 1.65 wt% Ca, 2.38 wt% Fe, 1.28 wt% Hf, 0.16 wt% Th and 0.61 wt% U (Fig. 4d).
Fergusonite	(Nb, Y, Ta, U, Al, Mg, Fe, REE)	Dark brown, tabular prismatic crystals.	44.28 wt% Ti, 16.93 wt% Nb, 1.55 wt% Ta, 9.11 wt% Si, 7.33 wt% Y, 3.77 wt% Th and 8.60 wt% U (Fig. 4e).
Samarskite	((Y, Ce, U, Fe)$_3$ (Nb, Ta, Ti)$_5O_{16}$)	Black to dark brown color, the grain are irregular to massive with a sub-conchoidal fracture (Fig. 4f).	49.25 wt% Nb, 14.46 wt% U, 3.13 wt% Ta and 12.49 wt % Pb (Fig. 4f).
Ishikawaite	((U, Fe, Ca, Y, Th) (Nb, Ta, Ti)$_2$ O_6)	Black, massive, euhedral to subhedral crystals with resinous to vitreous luster. Two phases are recorded: primary euhderal, and a replacement with columbite minerals.	19.92 wt% U, 4.71 wt% Fe, 1.16 wt% Ca, 12.71 wt% Y, 3.74 wt% Th, 30.50 wt% Nb, 3.82 wt% Ta and 13.72 wt % Ti (Fig. 4g).
Fluorite	(CaF_2)	Colorless, pale violet and/or dark violet, subhedral crystals (Fig. 4h).	50.51 wt % Ca, 47.28 wt% F and 2.78 wt% Y (Fig. 4h).

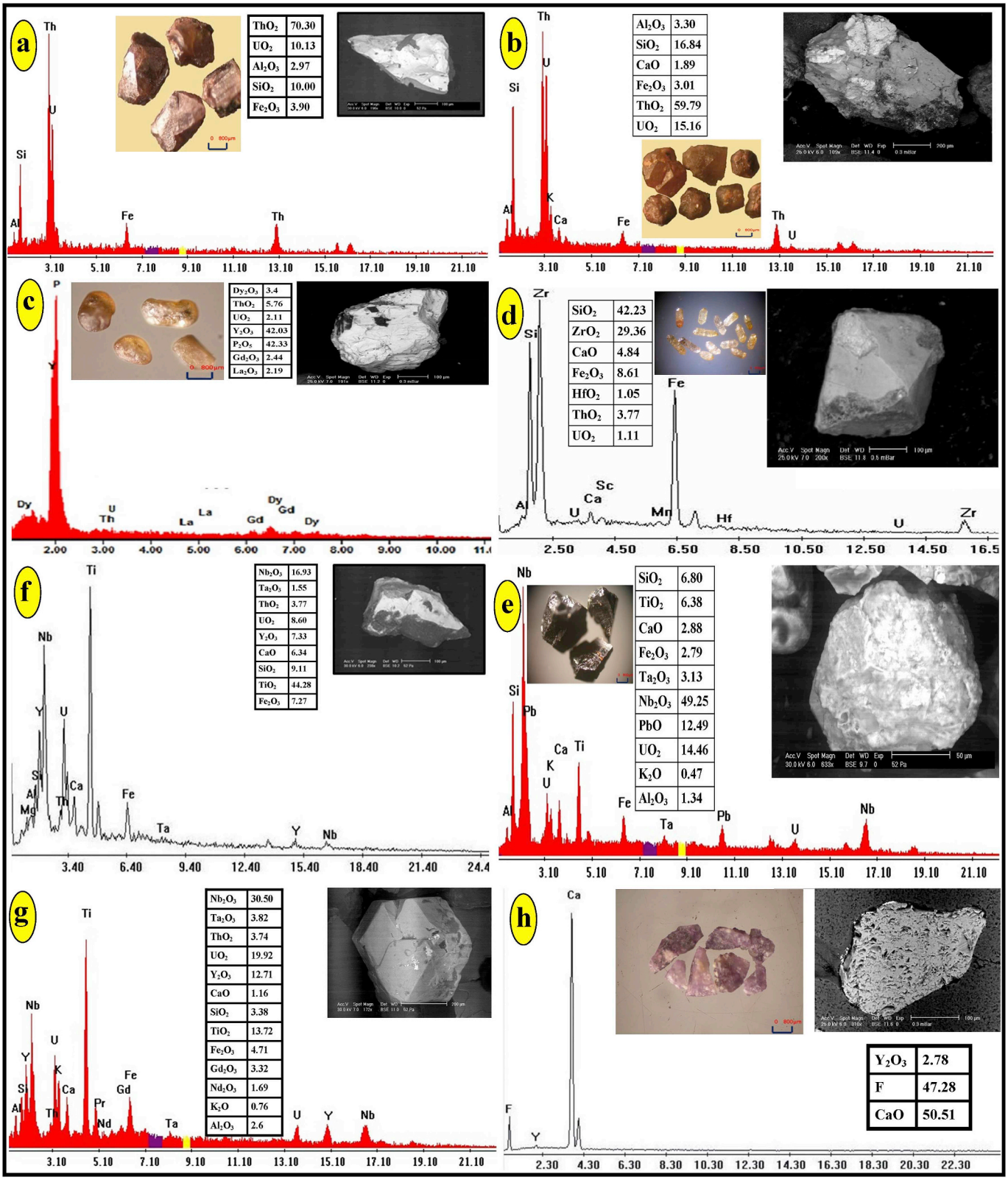

Fig. 4. Binocular microscope photos, SEM images and EDX analysis of a) Thorite, b) Uranothorite, c) Monazite, d) Zircon, e) Fergusonite, f) Samarskite, g) Ishikawaite and h) fluorite from the studied pegmatites of G. El Fereyid.

compared to the average of the host El Fereyid granite (Tables 2 and 3). They are characterized by enrichment of large ion lithophile elements (LILE; Pb, Rb, Sr) and high field strength elements (HFSE; Y, Zr, Th, U, Nb) and depletion in K, P and Ti, notably, Nb (av. 459.00 ppm) and Zr (av. 314.27 ppm). The other trace elements show also high average values such as Li (av. 452.32 ppm), Y (av. 52.41 ppm), Hf (av. 15.0 ppm), Th (av. 96.01 ppm) and U (av. 25.52 ppm) (Table 2). The chalcophile elements, especially Pb (av. 95.13 ppm) and Zn (av. 304.45 ppm) are also enriched along the pegmatite samples (Table 2). Gallium displaying high average value (50.20 ppm) compared to El

Table 2
Chemical composition of thirteen studied pegmatite samples from G. El Fereyid, South Eastern Desert, Egypt using ICP-MS. Value of Eu anomaly is calculated by: $Eu/Eu^* = [(Eu_N)/(SQ_R(Sm_N.Gd_N)]$; value of Ce anomaly is calculated by: $Ce/Ce^* = [(Ce_N)/(SQ_R(La_NPr_N)]$ (Worral and Pearson, 2001).

Rock type	Pegmatites													
S. No.	P1	P2	P3	P4	P5	P6	P7	P8	P9	P10	P11	P12	P13	Av.
Major oxides (Wt.%)														
SiO_2	77.01	73.89	76.18	74.82	76.5	76.39	74.92	75.72	75.62	75.97	75.83	75.54	73.85	75.56
TiO_2	0.06	0.04	0.19	0.17	0.09	0.03	0.09	0.04	0.15	0.02	0.04	0.02	0.09	0.08
Al_2O_3	10.6	12.95	11.36	12.36	11.77	11.45	12.75	11.98	12.17	12.34	11.15	12.36	12.98	12.02
Fe_2O_3*	1.57	2.33	2.46	1.9	1.84	1.03	1.82	1.74	1.82	1.9	2.67	2.14	1.85	1.93
Feo	2.02	3.00	3.16	2.44	2.37	1.33	2.34	2.24	2.34	2.44	3.43	2.75	2.38	2.48
MnO	0.02	0.02	0.05	0.04	0.1	0.02	0.1	0.01	0.1	0.02	0.12	0.13	0.03	0.06
MgO	0.15	0.15	0.45	0.43	0.07	0.05	0.07	0.07	0.03	0.03	0.07	0.02	0.06	0.13
CaO	0.34	0.22	0.13	0.18	0.34	0.18	0.32	0.21	0.09	0.06	0.08	0.01	0.18	0.18
Na_2O	3.99	4.77	3.7	4.03	3.24	4.46	3.99	4.57	4.26	4.97	4.13	5.11	4.08	4.25
K_2O	3.6	3.86	4.43	4.55	4.75	4.01	4.3	3.85	4.66	4.1	4.2	4.22	4.84	4.26
P_2O_5	0.01	0.01	0.04	0.04	0.01	0.01	0.04	0.04	0.01	0.01	0.01	0.01	0.04	0.02
L.O·I	1.65	1.49	0.81	1.08	1.02	1.37	1.40	1.80	0.89	0.41	1.30	0.44	1.6	1.20
Total	99.00	99.73	99.80	99.60	99.73	99.00	99.80	99.63	99.80	99.83	99.60	99.99	99.60	
Trace elements (ppm)														
U	41	16.9	17.3	40.9	6.9	44.6	30.9	5.8	33.9	13.3	21.8	28.5	31	25.52
Th	167.1	100.9	31	90.7	60.3	85.8	109.5	22	119.6	34.3	101.5	215.2	110.6	96.04
Cr	11	9	11	7	10	6	8	7	10	6	9	17	11	9.83
Y	21.3	80.9	180.4	19.8	89.9	13.2	26.5	26.9	23.9	20	27.5	20.6	130.5	52.42
Nb	696.62	180.9	151.41	450.62	198.43	532.45	190.84	180.94	366.79	448.96	610.63	1425.36	532.61	458.99
Zr	440.8	233.9	152	163.9	133.2	390.3	255.1	285.8	365.8	291	554.1	428.8	390.8	314.27
Ni	5.1	4.6	6.3	5.1	2.5	3.2	3.8	3.1	4.8	2.8	3.6	5.7	6.1	4.36
Ba	84	255	187	100	239	72	80	55	190	52	50	71	235	128.46
Pb	17.86	36.22	31.39	15.07	259.85	16.17	18.35	9.34	244.5	11.35	35.22	536.36	8.69	95.41
Rb	442	458	627.7	575	995.2	475	522.9	530.8	599	571.2	880.1	898.8	330.8	608.19
Sr	25	36	78	22	48	17	22	16	66	18	7	23	55	33.31
Zn	81.3	122.5	428	122.9	183.7	67.6	91.3	100.8	263.9	116.3	345.4	1770.7	263.5	304.45
Cu	40.6	9.8	13.9	26.5	36.3	39.1	13.3	16.2	13.5	31.1	6.6	536	30.6	62.58
V	7	3	14	1	2	2	7	3	12	< 1	1	< 1	2	5.00
Cs	1.9	1.8	6.2	5.9	3.5	1.8	3.6	2.9	3.9	2.8	5.3	2.4	3.5	3.5
Be	3	7	8	3	5	3	5	4	8	4	3	1	4	4.46
Sn	24.7	8.6	18.6	80.1	95.1	18.8	32.8	7.9	30.7	23.7	33.8	50.2	87.3	39.41
Li	136.6	156.9	205.6	320.2	476.3	72.5	309.6	116.5	689.3	102	1619.2	690.2	985.3	452.32
Ta	90.4	18.9	13	84.9	16.4	71	19.9	15.2	63.8	49.1	79.9	171.4	70.9	58.83
Co	1.1	0.8	2.6	0.6	0.3	0.5	0.5	0.6	0.9	< 0.2	0.4	0.5	1.1	0.83
Hf	20.29	22.29	5.56	10.98	6.9	18.77	11.9	10.39	5.7	11.76	29.59	27.56	13.2	15.00
Ga	57.24	40.2	42.6	39.3	38.03	54.31	48.9	36.16	33.9	69.34	59.3	65.45	40.9	50.20
Rare earth elements (ppm)														
La	9.6	8.9	20.9	8.9	18.8	9.3	6.8	5.1	17.3	2.6	5.7	2.4	6.9	9.48
Ce	43.38	44.62	95.87	35.97	48.88	39.35	60.5	23.85	30.88	14.22	28.97	12.13	75.19	39.35
Pr	4.1	7.5	10.3	6.1	6.1	4.6	5.9	2.8	6.1	1.7	3.7	1.5	8.9	5.15
Nd	10.3	20.8	30.7	20.8	20.8	10.3	10.3	6.3	29.9	3.3	8.2	3.1	25.39	14.54
Sm	2.5	2.4	10.1	5.4	5.4	2.6	1.1	1.7	0.9	1.1	2.3	0.9	5.9	2.96
Eu	< 0.1	0.3	0.4	0.3	0.3	< 0.1	0.3	< 0.1	0.4	< 0.1	< 0.1	< 0.1	0.4	0.22
Gd	1.4	4.6	8.6	4.6	4.6	1.1	5.6	1.1	1.4	0.6	1.1	0.7	6.8	3.18
Tb	0.4	0.5	2.7	1.3	1.3	0.5	2.1	0.4	0.2	0.4	0.5	0.3	1.5	0.93
Dy	3.6	4.7	21.5	10.2	10.2	3	10.6	3.6	9.8	3	4.7	3.5	11.6	8.47
Ho	1.1	1	5.8	2.5	2.5	0.9	0.9	1	2.9	1	1.4	1.1	1.4	1.68
Er	5.3	5.9	20.5	9.8	9.8	4.1	11.3	3.9	12.4	3.9	5.5	5.9	19.5	8.76
Yb	13.5	5.9	27.2	20.1	20.1	9.2	14.9	6.9	13.4	7.1	13.4	15.6	27.2	14.46
Lu	0.3	0.3	0.3	0.3	0.3	0.3	0.3	0.3	0.3	0.3	0.3	0.3	0.3	2.44
Tm	1.4	1.4	4.1	2.8	2.8	1	1.4	1	1	0.9	1.6	1.7	2.8	1.8
Geochemical Parameters														
Zr/Hf	21.72	10.49	27.34	14.93	19.30	20.79	21.44	27.51	64.18	24.74	18.73	15.56	29.61	24.30
Zr/Sr	17.63	6.50	1.95	7.45	2.78	22.96	11.60	17.86	5.54	16.17	79.16	18.64	7.11	16.60
Rb/Zr	1.0	1.96	4.13	3.51	7.47	1.22	2.05	1.86	1.64	1.96	1.59	2.10	0.85	2.40
Rb/Sr	17.68	12.72	8.05	26.14	20.73	27.94	23.77	33.18	9.08	31.73	125.73	39.08	6.01	29.40
Nb/Ta	7.70	9.6	11.6	5.3	12.10	7.5	9.6	11.90	5.8	9.1	7.6	8.30	7.5	8.7
Yb/Ta	0.15	0.31	2.09	0.16	1.23	0.13	0.75	0.45	0.21	0.14	0.17	0.09	0.38	0.5
Th/U	4.08	5.97	1.79	2.22	8.74	1.62	3.54	3.79	3.53	2.58	4.66	7.55	3.57	4.15
Ba/Rb	0.19	0.56	0.30	0.17	0.24	0.15	0.15	0.10	0.32	0.09	0.06	0.08	0.71	0.2
Eu/Sm	0.04	0.13	0.04	0.06	0.06	0.04	0.27	0.06	0.44	0.09	0.04	0.11	0.07	0.1
K/Rb	67.61	69.96	58.59	65.69	39.62	70.08	68.26	60.21	64.58	59.59	39.62	38.98	121.46	63.4
Rb/Ba	5.26	1.80	3.36	5.75	4.16	6.60	6.54	9.65	3.15	10.98	17.60	12.66	1.41	6.8
K/Ba	355.77	125.7	196.66	377.71	164.98	462.34	446.19	581.09	203.60	654.56	697.31	493.40	170.97	379.20
ΣREEs	90.55	104.9	244.36	102.66	79.57	87.65	135.0	58.85	130.18	41.02	79.57	51.53	193.18	113.44
ΣLREEs	61.65	75.95	149.86	53.06	100.28	66.25	48.97	39.85	85.48	23.02	48.97	20.13	122.68	71.70
ΣHREEs	28.90	29.0	94.50	49.60	54.90	21.40	30.60	19.0	44.70	18.0	30.60	31.40	70.50	41.74
ΣLREEs /ΣHREEs	2.13	2.62	1.59	1.07	1.83	3.10	1.60	2.10	1.91	1.28	1.60	0.64	1.74	1.79
Eu/Eu*	0.16	0.28	0.13	0.12	0.18	0.18	0.37	0.22	1.09	0.38	0.19	0.39	0.19	0.30

(*continued on next page*)

Table 2 (*continued*)

Rock type	Pegmatites													
S. No.	P1	P2	P3	P4	P5	P6	P7	P8	P9	P10	P11	P12	P13	Av.
Ce/Ce*	1.34	1.06	1.27	1.20	1.10	1.45	2.30	1.52	0.72	1.63	1.52	1.54	2.31	1.46
TE_1	1.66	1.66	1.53	1.56	1.20	1.89	3.10	1.98	0.83	2.31	2.08	2.15	2.68	3.92
TE_3	1.07	0.79	1.19	3.07	1.19	1.36	2.32	1.26	0.77	1.56	1.36	1.29	1.49	1.44
$TE_{1.3}$	1.33	1.14	1.35	2.19	1.19	1.60	2.68	1.58	0.80	1.90	1.68	1.66	2.0	2.29

Table 3
Chemical composition of seven selected monzogranite samples from G. El Fereyid, South Eastern Desert, Egypt using ICP-MS.

Rock type	Monzogranite						
S. No.	M1	M2	M3	M4	M5	M6	M7
Major oxides (Wt.%)							
SiO_2	70.4	70.88	72.24	70.98	70.35	70.79	72.36
TiO_2	0.42	0.4	0.43	0.44	0.43	0.93	0.42
Al_2O_3	15.1	15.61	14.42	15.38	14.92	14.92	14.59
Fe_2O_3*	2.44	2.45	2.17	2.15	3.17	2.35	2.07
FeO	2.20	2.20	1.95	1.93	2.85	2.11	1.86
MnO	0.023	0.034	0.061	0.065	0.059	0.064	0.058
MgO	0.82	0.66	0.8	0.75	0.81	0.8	0.7
CaO	1.44	1.3	0.9	1.16	1.45	1.41	1.27
Na_2O	4.22	3.8	4.33	4.04	4.47	4.16	4.57
K_2O	3.89	4.41	4.08	4.38	3.76	4.51	3.32
P_2O_5	0.14	0.11	0.23	0.21	0.24	0.15	0.24
L.O·I	0.41	0.35	0.34	0.35	0.34	0.46	0.4
Total	99.28	100.00	100.00	99.90	99.99	100.54	99.99
Trace elements (ppm)							
U	3.8	2.9	2.2	2.1	2.5	2.7	2.2
Th	15.9	24.6	11.7	9.8	13	20.6	20.3
Cr	222	162	202	190	193	115	264
Y	26.5	40.9	23.7	23.4	21.1	46.1	22.3
Nb	14.23	9.9	9.11	8.7	7.95	16.3	8.45
Zr	40	39.8	41.5	37.1	46	35.2	45.8
Ni	87.9	88.9	124.5	113.5	111.7	63.7	162.1
Ba	897	695	861	986	814	833	698
Pb	66.1	70.2	39.73	60.78	50.91	148.24	45.6
Rb	120.6	130.5	85.8	98.5	90.4	131.7	81.7
Sr	285	285	278	276	287	239	270
Zn	847.3	579.8	426.1	847.8	559.8	2267.7	524.9
Ti	0.63	0.55	0.47	0.56	0.52	0.74	0.45
Cu	1474.6	2255.6	708.2	1448.3	962.8	3835.6	886
V	31	38	32	33	32	31	31
Cs	1.2	1.3	0.8	1.2	1.2	3.6	1.4
Be	2	2	2	2	2	2	2
Sn	23.3	30.8	11.6	21.6	15	52.6	13.7
Li	24.6	33.6	20	24.1	22.4	34.5	26.5
Ta	0.8	0.7	0.7	0.7	0.6	1.4	0.6
Co	7.6	10.1	8.5	8.5	8.1	6.9	8.9
Hf	1.87	2.9	1.21	1.08	1.21	1.14	1.32
Ga	20.66	20.14	20.15	20.52	19.87	21.03	19.79
Rare earth elements (ppm)							
La	40.10	36.20	29.90	35.00	36.00	40.60	52.90
Ce	88.50	102.20	64.65	72.07	75.38	83.22	105.96
Pr	12.90	10.20	7.90	8.50	9.30	10.20	12.80
Nd	40.10	45.50	28.20	30.40	32.70	34.90	43.40
Sm	6.50	6.60	5.60	5.80	5.90	7.00	7.40
Eu	1.20	1.00	1.10	1.20	1.10	1.00	1.30
Gd	6.70	5.10	4.90	5.80	4.40	6.20	5.50
Tb	1.00	0.70	0.90	0.90	0.80	1.20	0.70
Dy	6.60	4.00	4.60	4.20	3.90	6.70	3.50
Ho	1.50	0.90	0.90	0.90	0.80	1.60	0.80
Er	4.70	2.00	2.40	2.60	2.10	4.80	2.40
Yb	5.1	2.00	2.5	2.30	2.00	5.2	2.6
Lu	0.8	0.3	0.4	0.4	0.3	0.8	0.4
Tm	0.8	0.4	0.4	0.4	0.3	0.8	0.4
Geochemical Parameters							
Zr/Hf	21.4	13.7	34.3	34.4	38.0	30.9	34.7
Zr/Sr	0.1	0.1	0.1	0.1	0.2	0.1	0.2

Table 3 (*continued*)

Rock type	Monzogranite						
S. No.	M1	M2	M3	M4	M5	M6	M7
Rb/Zr	3.0	3.3	2.1	2.7	2.0	3.7	1.8
Rb/Sr	0.4	0.5	0.3	0.4	0.3	0.6	0.3
Nb/Ta	17.80	14.1	13.0	12.4	13.30	11.6	14.10
Yb/Ta	0.2	2.9	3.6	3.3	3.3	3.7	4.3
Th/U	7.4	9.5	5.3	4.7	5.2	7.6	9.2
Ba/Rb	267.80	5.3	10.0	10.0	9.0	6.3	8.5
Eu/Sm	0.2	0.2	0.2	0.2	0.2	0.1	0.2
K/Rb	267.8	280.5	394.7	369.1	345.3	284.3	337.30
Rb/Ba	0.1	0.2	0.1	0.1	0.1	0.2	0.1
K/Ba	36.0	52.7	39.3	36.9	38.333	44.9	39.50
ΣREEs	216.50	217.00	154.35	170.47	174.98	204.22	240.06
ΣLREEs	189.30	201.70	137.35	152.97	160.38	176.92	223.76
ΣHREEs	27.20	15.30	17.0	17.50	14.60	27.30	16.30
ΣLREEs /ΣHREEs	6.96	13.18	8.08	8.74	10.98	6.48	13.73
Eu/Eu*	0.56	0.53	0.64	0.63	0.67	0.46	0.62
Ce/Ce*	0.94	1.28	1.01	1.01	0.99	0.98	0.98
TE_1	1.16	1.09	1.07	1.04	1.06	1.06	1.06
TE_3	0.89	0.86	1.07	0.94	1.04	0.99	0.82
$TE_{1.3}$	1.02	0.97	1.07	0.99	1.05	1.03	0.93

Fereyid monzogranite, which probably is not controlled by K-feldspar fractionation but is buffered by other phases. The large ion lithophile elements (LILE; Rb, Sr and Ba) show wide variations in composition when compared with the host granite (Tables 2 and 3). Barium is enriched (av. 128.46 ppm) and Rb is enriched (av. 608.19 ppm) while Sr (av. 33.31 ppm) is relatively constant (Table 2).

Concentration of trace element contents are compared with other pegmatites from Egypt (e.g. pegmatites of Abu Rusheid area, south Eastern Desert (Ragab, 2011) and Um Taghir El Tahtani, central Eastern Desert (Abdel Warith et al., 2007)). The studied pegmatites show higher content of trace elements (Nb, Rb, Li, Zr, Zn, Sr; Table 2). The pegmatites of Abu Rusheid area show Zr (30–583 ppm), Li (5–248 ppm), Rb (94–758 ppm), Nb (78–805 ppm), Pb (56–207 ppm), Ta (10–190 ppm), U (16–262 ppm) and Th (37–699 ppm) (Ragab, 2010). Whereas the pegmatites of Gabal Um Taghir El Tahtani shows Zr (av. 5954 ppm), Y (av. 563 ppm), Sr (av. 65 ppm), Rb (av. 71 ppm), Nb (av. 1569 ppm), Zn (av. 123 ppm), Ba (av. 181 ppm) (Abdel Warith et al., 2007).

The trace elements data for all pegmatite samples are normalized to the primitive mantle (Sun and McDonough, 1989) and compared with the average host granite on the spider diagram (Fig. 6). It shows trace element pattern similarities amongst the samples but with higher values compared to the host rock.

4.4.2. Rare earth elements geochemistry

Rare earth elements (REEs) geochemistry of the studied pegmatites (Table 2) show the total REEs ranging from 41.02 to 244.36 ppm, deducing that these pegmatites are depleted in REEs relative to the international range (250–270 ppm) of Hermann (1970). ΣLREES in the pegmatites range from 20.13 to 149.86 ppm with average 71.70 ppm, while ΣHREEs range from 18.0 to 94.50 ppm with average 41.74 ppm.

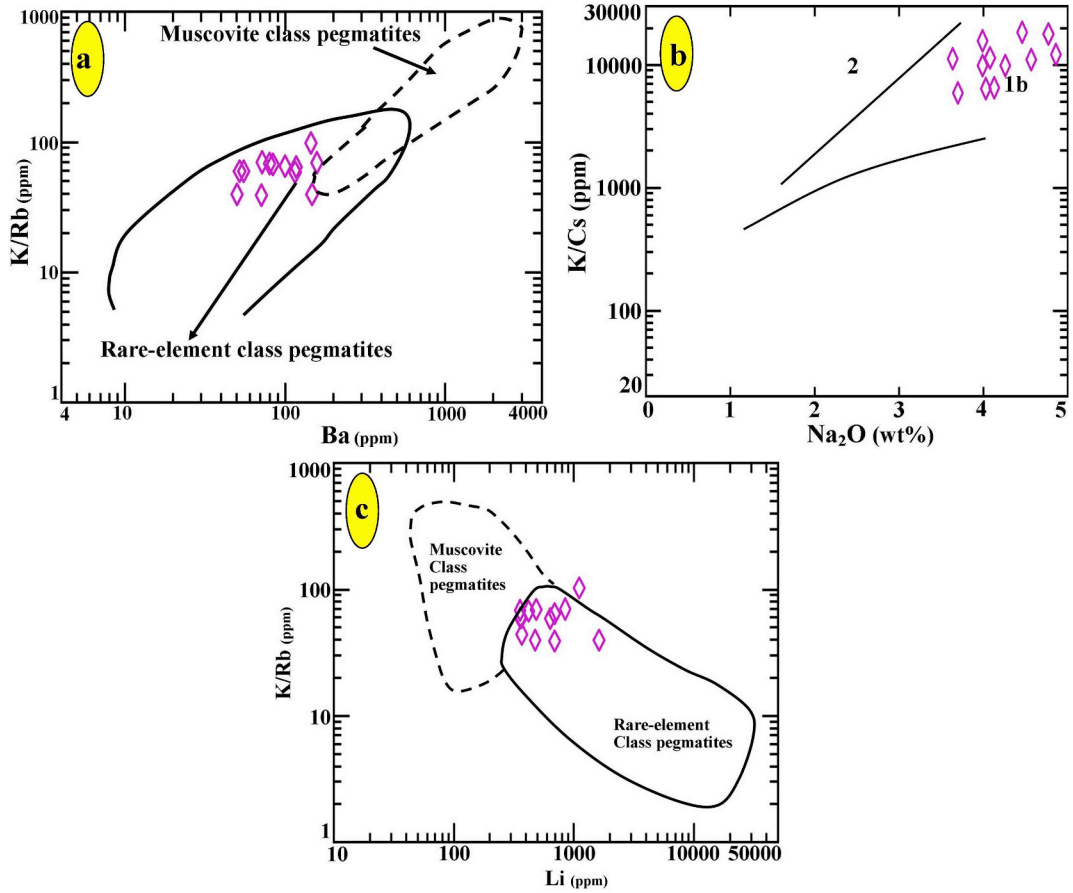

Fig. 5. a) Na_2O vs K/Cs diagram showing boundaries between mica-bearing (2), and rare element–bearing pegmatites (1a = Cs-bearing; 1b = Li-bearing without Cs) according to Gordiyenko (1971) as presented in Trueman and Černý (1982), b) Ba vs K/Rb diagram according to Mehnert and Busch (1981) and c) Li vs K/Rb diagram according to Černý and Burt (1984).

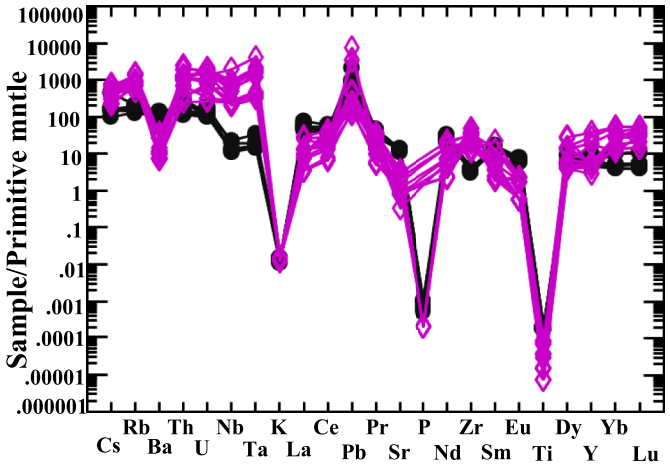

Fig. 6. Multi-elements patterns of the pegmatite samples normalized to the primitive mantle values (Sun and McDonough, 1989).

Where compared with pegmatites of other areas in the Eastern Desert of Egypt (e.g. Abu Rusheid area (Ragab, 2011)), the studied pegmatites show only higher contents in Pr, Nd and Sm (Table 2). The pegmatites of Abu Rusheid area show higher content of rare earth elements: i.e., La (1.1–26.70 ppm), Ce (4.93–113.32 ppm), Pr (0.60–3.50 ppm), Nd (1.80–8.8 ppm), Sm (0.8–9.30 ppm), Eu (0.1–0.8 ppm), Gd (0.8–12.1 ppm), Tb (0.4–4.90 ppm), Dy (4.40–53.10 ppm), Ho (1.2–5.7 ppm), Er (5.20–23.90 ppm), Tm (1.10–12.40 ppm), Yb (9.70–111.1), Lu (1.40–16.50 ppm). From the REE data and according to Cullers and Graf (1984), the pegmatites of the investigated area show high negative Eu anomaly (Fig. 7). The studied samples have an average Eu/Sm = 0.08 and LREEs/HREEs = 0.88. Normalized REEs patterns relative to chondritic values (Fig. 7) of Boynton (1984) are distinguished by strong ΣLREEs enrichment and low ΣHREEs content because of the presence of some accessory minerals like monazite, apatite and zircon. In the studied pegmatite, the Eu/Eu* values show negative anomaly, and the Ce/Ce* values show highly positive anomaly (Fig. 7) relative to host rock (Tables 2 and 3).

4.4.3. REE tetrad effect

Fractionation of minerals alone can't explain non-CHARAC (Charge-and-Radius-Controlled) behavior of Zr and Hf, Y and Ho (Bau, 1996, 1997). Accordingly, it is deduced that tetrad effect and highly fractionated trace element ratios of Y/Ho and Zr/Hf give an indication that a trace element behavior is similar to that in aqueous system. The term 'tetrad effect' (Masuda et al., 1987) refers to subdivision of the 15 lanthanide elements into four groups in a chondrite normalized distribution pattern and each group forms a smooth convex (M-type) or concave (W-type) pattern. The values of tetrad effect are calculated according to Irber (1999) quantification method:

$Ce^* = Ce_N/La_N^{2/3}xNd_N^{1/3}$), $Pr^* = Pr_N/(La_N^{1/3}xNd_N^{2/3})$, $Tb^* = Tb_N/(Gd_N^{2/3}xHo_N^{1/3})$, $Dy^* = Dy_N/(Gd_N^{1/3}xHo_N^{2/3})$, $TE_3 = (Tb^*xDy^*)^{1/2}$, $TE_1 = (Ce^*xPr^*)^{1/2}$ and $TE_{1.3} = (TE_1xTE_3)^{1/2}$

REE tetrad effect was mainly observed in late magmatic differentiation and mainly related to strong hydrothermal interactions (Jahn et al., 2001). For the studied pegmatite samples, values of tetrad effect have an average of 1.62 (Table 2). The M-shaped pattern shows $TE_{1.3}$ >

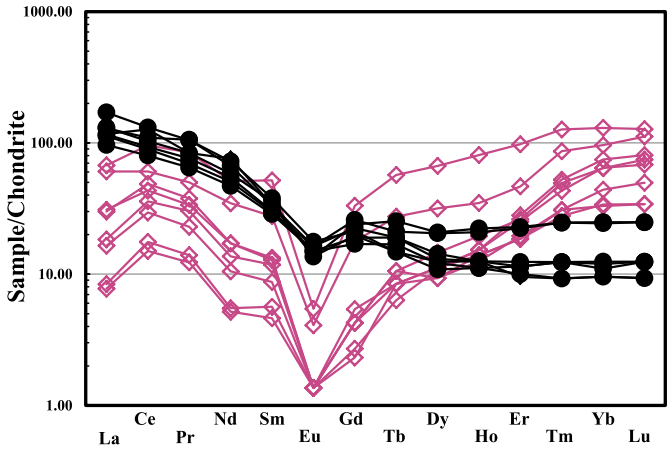

Fig. 7. Rare Earth Element distribution pattern of pegmatite samples normalized to chondrite of Boynton (1984).

1.1 and the W-shaped $TE_{1.3} < 0.9$ (Masuda et al., 1987). Whereas, the REE pattern that does not show a tetrad effect has values of $TE_{1.3} < 1.1$ (Masuda et al., 1987). Accordingly, the Chondrite-normalized REE patterns of the studied pegmatite samples show M-type tetrad effect (Fig. 7), where the values of $TE_{1.3}$ are more than 1.1 (Table 2).

4.4.4. Uranium and thorium geochemistry

Uranium and thorium contents have a wide range in all investigated pegmatites (Table 2) but with relatively lower concentrations compared with the other pegmatites from other areas of Egypt (e.g., Abu Rusheid area (Raslan and Ali, 2011; Ragab, 2011)). Uranium is ranging from 5.8 ppm to 44.6 ppm, which is higher than the average 2.4 ppm of El Fereyid monzogranite (Tables 2 and 3). Also, concentrations of thorium show a wide range from 22 ppm to 215.2 ppm, which are also higher than the average 17.2 ppm of El Fereyid monzogranite (Tables 2 and 3). This wide range is depending mainly upon the abundances of U–Th-bearing minerals (thorite, uranothorite, zircon and fergusonite) in the pegmatite. The Th/U ratios are ranging from 1.79 to 8.74 in the pegmatite samples. A positive correlation is between U and Th (Fig. 8a), and a highly positive relationship between Zr–Th and Zr–U was also recorded (Fig. 8b and c).

4.5. Gamma ray spectroscopy and radiometric investigations

For regional in-situ field radiometric measurements using a portable four-channel (dose rate (D.R.), K, eU, and eTh), gamma-ray spectrometer Model RS-230 was accomplished along Gabal El Fereyid monzogranites and their associated pegmatites. The resulted radiometric data were treated statistically (Table 4) to know the distribution characteristics of radioelements and their ratios in the various rock types in the study area (Figs. 9 and 10). The field radiometric measurements revealed localization of radiometric anomaly associated with the granitic pegmatites encountered within monzogranites. These measurements show that eU reaches up to 6.0 ppm in the monzogranite samples, and up to 150.0 ppm in the pegmatite samples. Whilst, eTh reaches up to 29.0 ppm in the monzogranite samples, and up to 377.0 ppm in the pegmatite samples. The statistical treatment of spectrometric data is shown on binary diagrams of eTh against eU, eU against eU/eTh and eU against eU-eTh/3.5 (Figs. 9 and 10). From these results, the monzogranite shows weak enrichment by U-mineralization, whereas the pegmatite hosts high uranium content.

5. Discussion

5.1. Mineralogical and geochemical implications of granitic pegmatites

The mineralogical and geochemical characteristics especially those of rare earth elements are good proxies for indication of the genesis and physicochemical conditions for the formation of the of the studied granitic pegmatites. These studies lead us to conclude that these granitic pegmatites and their associated uranium, thorium and rare metals mineralization are magmatic in origin with a hydrothermal input. The magmatic mineralization is evidenced by occurrence of thorite and zircon, whereas the hydrothermal activity is represented by

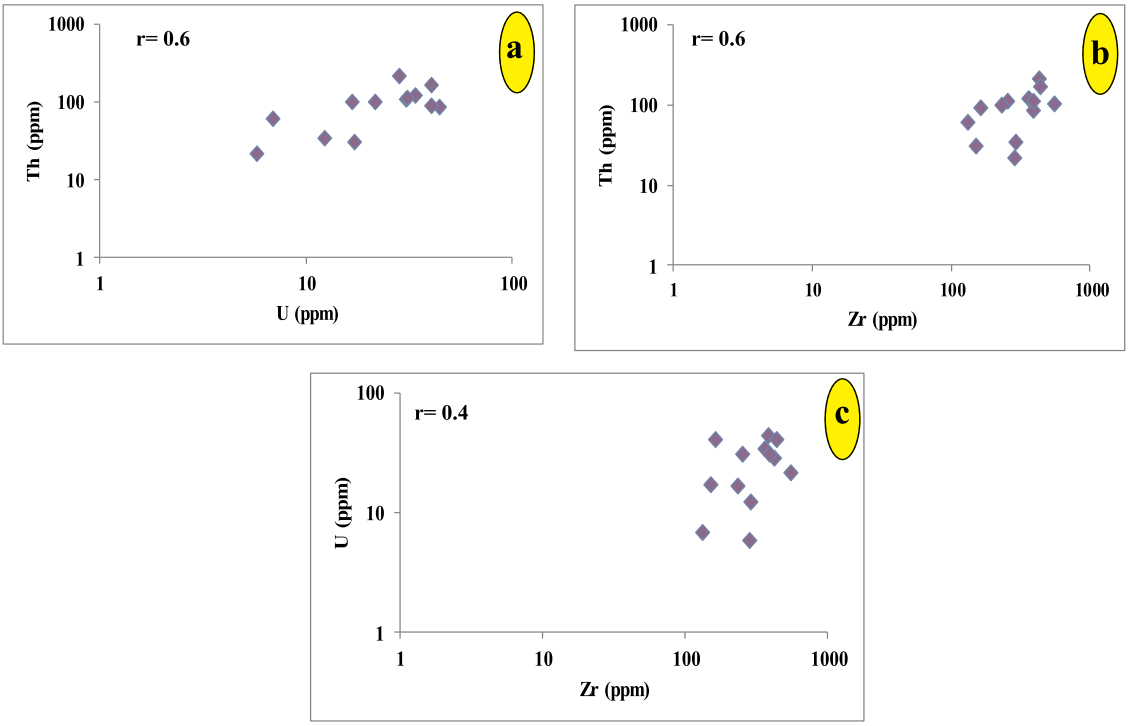

Fig. 8. Log-log variation diagrams of the studied pegmatite samples between (a) U–Th, (b) Zr–Th and (c) Zr–U.

Table 4
Data of radiometric measurements for the studied monzogranite and their associated pegmatites, G. El Fereyid area.

	D.R.(mv/y)	K%	eU(ppm)	eTh(ppm)	eU/eTh	eTh/K	eU-(eTh/3.5)
Monzogranite							
Mean(X)	12.0	4.0	3.2	12.3	0.3	3.6	−0.3
Standard deviation (S)	7.0	1.0	0.8	4.0	0.1	1.2	1.2
Minimum	7.2	2.0	1.1	4.2	0.1	1.0	−5.0
Maximum	104.0	6.2	6.0	29.0	1.0	7.0	3.0
X+3S	32	6	5.6	24.0	1.0	7.2	3.3
X-3S	−9.0	1.2	1.0	1.0	0	0	−4.0
No. of Reading	200						
Pegmatites							
Mean(X)	655.1	5.0	38.0	116.0	0.4	27.0	4.8
Standard deviation (S)	548.4	1.0	33.0	99.0	0.2	24.0	22.0
Minimum	9.4	2.1	1.2	2.0	0.1	0.3	−66.1
Maximum	1800.0	7.1	150.0	377.0	1.5	114.0	88.0
X+3S	2300.3	7.6	137.0	412.4	1.0	99.0	70.2
X-3S	−990.1	1.6	−61.1	181	−0.2	−45.0	−61.0
No. of Reading	180						

alteration of feldspars and formation of pyrite and iron oxides associated with the radioactive minerals.

By plotting barium content against K/Rb ratio of pegmatite samples (Fig. 5b), they show an increase in Ba content with increasing K/Rb ratio. Therefore, the barium content is an important indicator of the fractionation degree of a pegmatite (Mehnert and Busch, 1981).

Hf is enriched with respect to Zr (low Zr/Hf ratio) in the zircons that are mostly related to the late stages of pegmatite crystallization (Owen, 1987; Uher and Černý, 1998). Wang et al. (2010) interpreted the lower Zr/Hf ratio in granitic zircon by lower crystallization temperature. Also, the lower Zr/Hf ratio is a good parameter for the crystallization of hydrothermal zircon (Caironi et al., 2000).

Positive correlation between U and Th (Fig. 8a) is mostly an indication about the linkage between the two elements and accommodation with their bearing minerals. The highly positive relationship between Zr–Th and Zr–U (Fig. 8b and c) is also an indication that U and Th enrichment is mainly controlled by abundance of zircon in the samples, whereas the other U–Th-bearing phases (fergusonite-Y) are present in low amount compared to zircon (Abu Steet et al., 2018).

According to the classifications of granitic pegmatites, particularly those enriched in rare earth elements, done by Černý (1991) and Černý and Ecrit (2005), two classes: i.e., NYF (Niobium–Yttrium–Fluorine family that is enriched in Nb, Y, and F ± Be, REE, Sc, Ti, Zr, Th, and U) and LCT (Lithium–Cesium–Tantalum family with dominant accumulation of Li, Cs, Ta, Rb, Be, Sn, B, P and F) were described. From trace elements geochemistry, the studied granitic pegmatites could be classified as NYF pegmatites. As well, decreasing Nb/Ta ratio is typical for NYF granitic pegmatites (Černý et al., 1986; Černý, 1990, 1991).

5.2. Uranium and thorium radioactivity

The wide ranges of eU/eTh ratio of granitic pegmatites (1.0–1.5) and eTh/K ratio (0.3–113.5) indicate that they have a very high U potential mobilization and its ratios is not normal and form anomalous zones (Saleh et al., 2018).

The eTh/eU diagram of the studied monzogranite and their associated pegmatites (Figs. 9 and 10) shows an enrichment of uranium where the highest eU and eTh values are for the pegmatite samples. Most of the samples are in between 3.0 and 6.0 eTh/eU ratio with a simultaneous increase in both eU and eTh. Uranium remained relatively immobile in the original rock. According to this model, the radioelement increases gradually during magmatic fractionation, but the ratio changes due to different alteration processes (Saleh et al., 2018; Heikal et al., 2018, 2019; Heikal and Top, 2018).

Most of the studied monzogranite and pegmatite samples have higher uranium content (Table 4) than that of the hypothetical uranium distribution (Figs. 9 and 10) and so the mobilization gives positive values, which in turn indicates that U of these samples is leaching in (Cambon, 1994).

5.3. Mobilization and migration of uranium and thorium

Uranium is the most expected element to be mobilized, due to its geochemical behavior and nature of its hosting rocks; its mobilization is discussed through two main topics; 1) eU/eTh ratio and 2) type and amount of mobilization.

5.3.1. eU/eth ratio

The commonly recorded eU/eTh ratio for the granitic rocks is about 0.33 (Clark et al., 1966; Rogers and Adams, 1969; Stuckless et al., 1977; Boyle, 1982). That ratio is considered as an important radiometric indicator to identify the fate and proximity of the U-mineralization. However, the enrichment of uranium could be indicated by increasing this ratio above 0.33 while the depleted or initially uranium poor granites could be indicated by decreasing the ratio than 0.33. The value of eU/eTh ratio in the productive uraniferous rocks is generally ≥1 (Darenely and Ford, 1989). The eU/eTh ratio for each rock type is quoted in (Table 3). The averages of the eU/eTh ratio are 0.4 for monzogranite and pegmatite, indicating uranium addition.

The radiometric studies of anomalous pegmatite samples show that their equivalent uranium contents (eU) range from 1.2 to 150 ppm while their equivalent thorium contents (eTh) vary from 2.0 to 377 ppm. In contrast, the eU and eTh contents of El Fereyid monzogranites range from 1.1 to 6.0 ppm and from 4.2 to 29.0 ppm respectively. This indicates strong post-magmatic uranium enrichment in the pegmatitic melt. This could be supported by high concentration of uranium in accessory minerals (e.g., zircon, fluorite and radioactive-bearing mineral (e.g., fergusonite) and adsorbed mostly by iron oxides (Ali et al., 2008).

5.3.2. Type and amount of uranium mobilization

The uranium mobilization rate (P) is calculated by P = Um/Up x 100%. The obtained results of Uo, Um and P for representative samples of the studied rock units are listed in Table 5.

Dynamics of uranium-rich fluids and amount of mobilized uranium as well as uranium mobilization rate in the studied rocks are calculated through several steps using equations of Benzing Uranium Institute of China and CNNC (1993). The paleo-uranium background (the original uranium content) is calculated by Uo = eTh x eU/eTh, where: Uo is the original uranium content, eTh is the average of thorium content in certain geologic unit and eU/eTh is the average of the regional eU/eTh ratio in different geologic units. The average regional eU/eTh in the study area is 0.4.

The amount of the mobilized (migrated) uranium (Um) is calculated by Um = Up – Uo, where, Um is the amount of the mobilized uranium

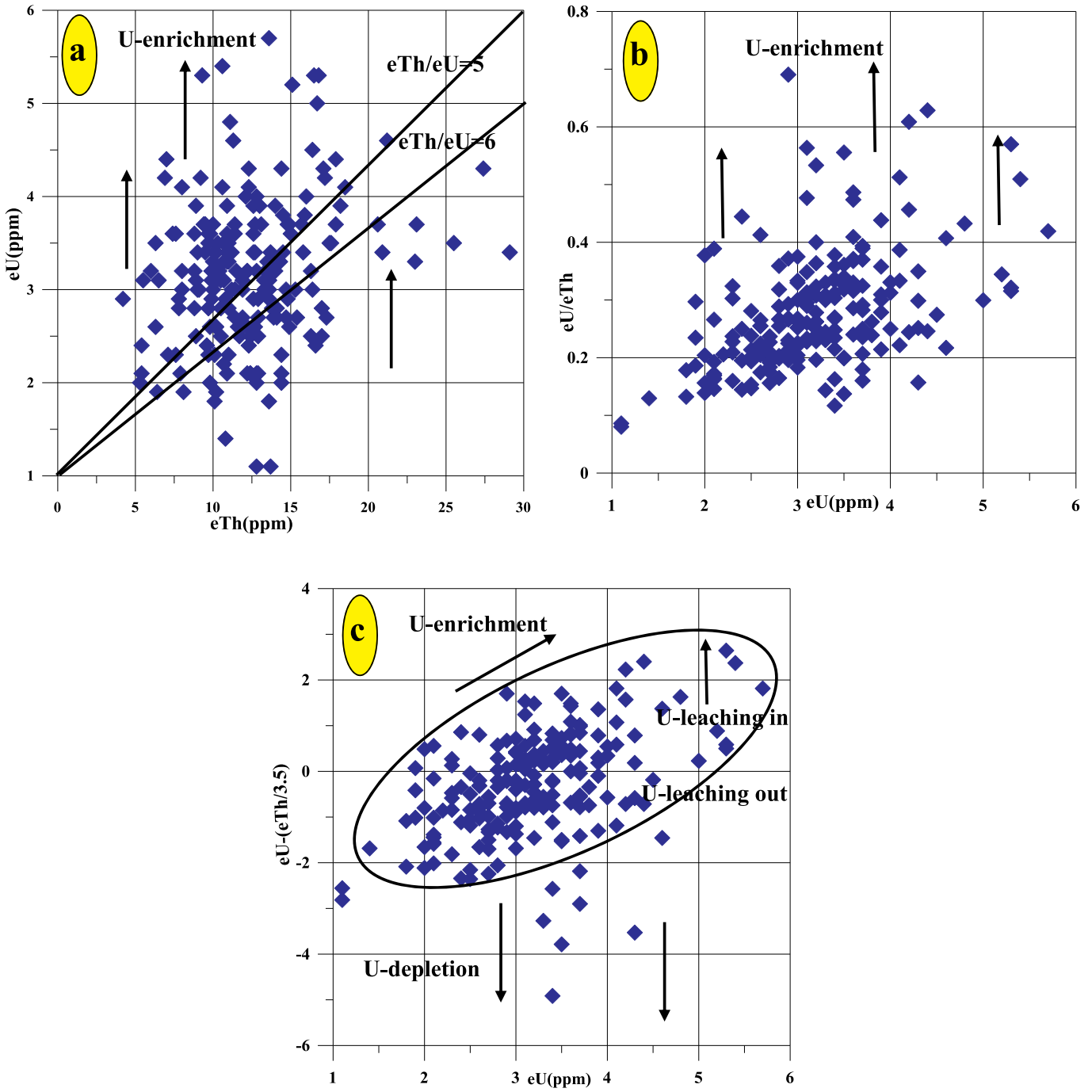

Fig. 9. Plots of radioactive elements for 200 ground gamma-ray spectrometry measurements of monzogranite at G. El Fereyid area.

and Up is the average of the present uranium content in certain geologic unit. If Um > 0: this means that U was gained or mobilized into the geologic body during late evolution (migration in). If Um < 0: this means that U had been lost from the geologic body during late evolution (migration out). The data reveals that the Um values are < 0 in monzogranites and pegmatites indicating that U was mobilized out from them (migration out), mostly to the stream sediments.

5.4. Mineralization potentiality

Based on the field and textural relations, mineralogical and geochemical data, the studied pegmatites are consistent with fractional crystallization trend from granites toward pegmatites. They are distinguished by zoning structure (concentric layering) that is typical of highly fractionated and mineralized pegmatites (Sweetapple, 2000). The studied pegmatites were undergone high fractionation and concentration of rare elements and volatiles. From the collected data, El Fereyid pegmatites are mineralized as many Precambrian pegmatites in the Basement Complex of Egypt (e.g. pegmatites studied by Ali, 2007; Nossair, 1987; Mohamed et al., 1994 and Asran et al., 2013). These pegmatite bodies reveal an overall enrichment in HFSE concentrations, which behave incompatibly in silica-saturated alkaline magma. The mineralogical studies of El Fereyid pegmatites have provided evidences that thorite, uranothorite, zircon, fergusonite, samarskite and ishikawaite are the major U-, Th-, Nb- and REE-bearing minerals.

The trace elements analysis shows that the studied pegmatites

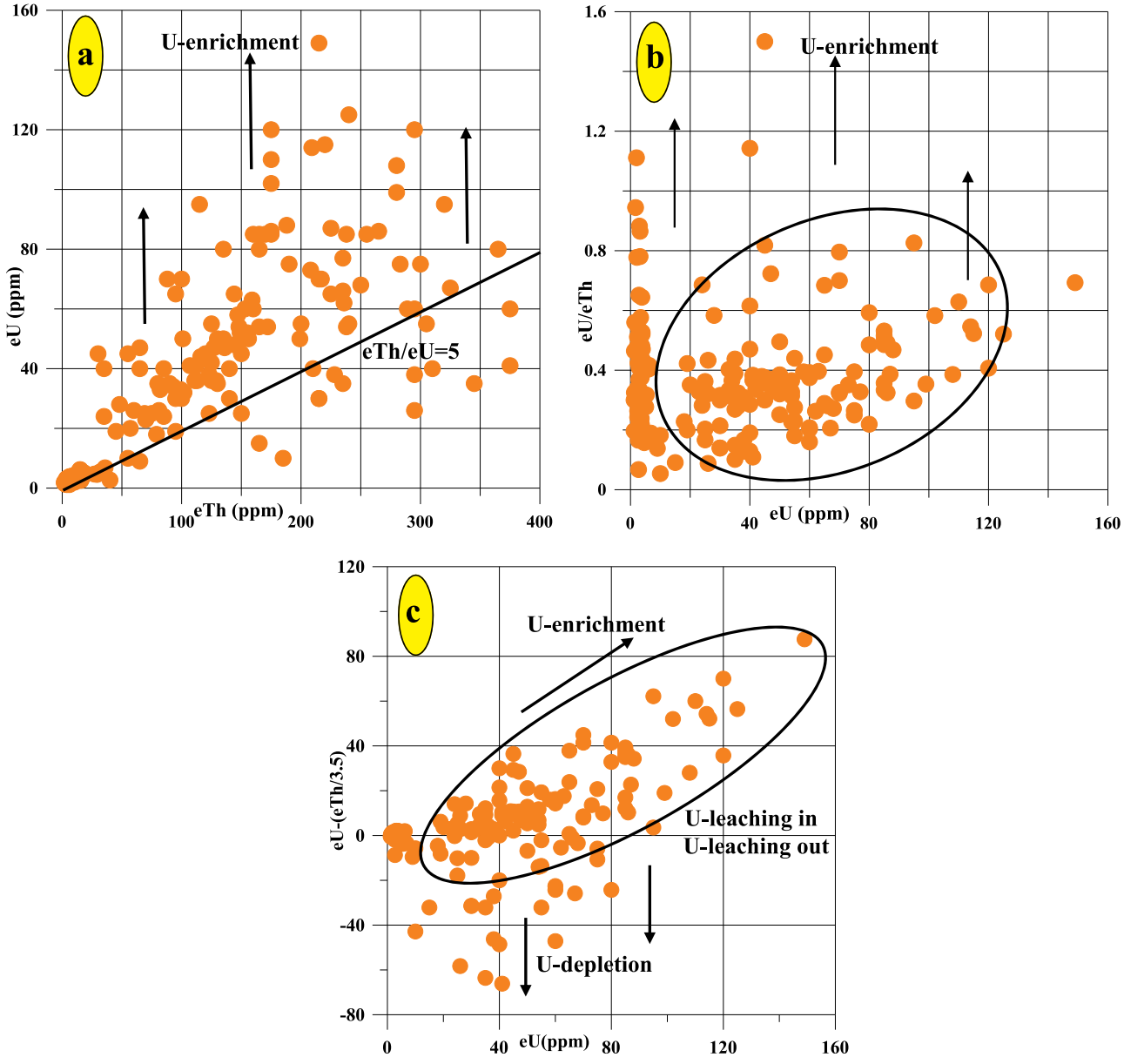

Fig. 10. Plots of radioactive elements for 180 ground gamma-ray spectrometry measurements of pegmatites at G. El Fereyid area.

Table 5
Average of original uranium, present uranium, mobilized uranium and uranium mobilization rate in the studied rocks.

Rock type	eTh (ppm)	Uo	Up	Um	P%
Monzogranites	12.3	4.92	3.18	−1.74	−54.72
Pegmatites	72.9	29.16	27.5	−1.66	−6.03

documents relatively high contents of Zr, Nb, U, Th and REE (Table 2). The trace element ratios support a high degree of fractionation in the evolutionary history of the pegmatites. These features agree with the moderately positive Ce signature and negative Eu anomaly REE pattern.

6. Conclusions

An approach was made to study the radioactive pegmatites to determine their compositional characteristics and assessing their mineralization potentials at El Fereyid area in the South Eastern Desert of Egypt. Economically important uranium and rare earth elements mineralization were recorded in the pegmatite bodies intruding monzogranites. These pegmatites occur as veins, pockets, dykes and irregular bodies. Petrographic studies of the pegmatites and their enclosing granitic rocks shows similar mineral composition mainly of perthite, quartz and less abundant plagioclase with minor accessory phases of micas.

Mineralogically, the studied pegmatites are characterized by abundance of radioactive minerals, radioelements-bearing accessory minerals and rare earth elements. Geochemically, they are clearly enriched in Zr, U, Th, Nb, F and REE compared to the host granite. They are considered as a promising ore material for their rare earth elements mineralization which contain mainly Zr, Ta, Y, U, Th, Zn, Nb, Rb, Hf, and REE. The overall geochemical signatures of El Fereyid pegmatites show high fractionation, and high level of rare earth elements mineralization potential. The main potentiality of the study area is in U and Th, whereas Nb, Y, Zr and REE are of secondary importance. The high levels of radioactivity and rare earth elements mineralization in some pegmatite bodies make them a target to enlarge the potentiality of the highly mineralized localities.

Acknowledgments

We would like to thank Prof. Dr. Masoud S. Masoud, Prof. Dr. A. Abdel-Gawad (Nuclear Materials Authority of Egypt) for their kind support and field facilities. Special thanks to Prof. Dr. Ehab Korany (Nuclear Materials Authority of Egypt) for his fruitful help in petrography. The authors are indebted to Prof. Dr. Read Mapeo, Editor-In-Chief of Journal of African Earth Sciences, and Prof. Dr. Mamdouh Abdeen, the Associate Editor, for reviewing and editing of the manuscript. Special thanks to Prof. Dr. Mohamed Th. Heikal and anonymous reviewers for their encouraging comments and annotations that greatly improved an earlier version of the manuscript.

Appendix A. Supplementary data

Supplementary data to this article can be found online at https://doi.org/10.1016/j.jafrearsci.2019.103651.

References

Abd El Naby, H.H., Saleh, G.M., 2003. Radioelement distribution in the proterozoic granites and associated pegmatites of gabal El Fereyid area, southeastern Desert, Egypt. Appl. Radiat. Isot. 59, 289–299.

Abdel-Karim, A.M., 1999. REE-rich accessory minerals in granites from Southern Sinai, Egypt: mineralogical, geochemical and petrogenetic implications. In: The 4th International Conference on Geochemistry. Alexandria University, Egypt, pp. 83–100.

Abdel Warith, A., Raslan, M.F., Ali, M.A., 2007. Mineralogy and radioactivity of pegmatite bodies from the granitic pluton of Gabal Um Taghir El-Tahtani area, central Eastern Desert, Egypt. In: The 10th International Mining, Petroleum, and Metallurgical Engineering Conference – March 6 – 8, 2007, pp. 15–30.

Abdel Karim, A.M., Sos, E.A., 2000. Geochemical characteristics and potassium argon ages dating of some granitoids from South Eastern Desert, Egypt. Egypt.J. Geol. Soc.Egypt. 44 (1), 305–318.

Abu Steet, A.A., El Sundoly, H.I., Abdel Hamid, A.A., 2018. Rare elements distribution and mineralization potentiality of pegmatites in gabal Abu samyuk granite, north Eastern Desert, Egypt. Egypt. J. Geol. 62 14pp.

Ali, B.A., 2007. Geochemistry of U-Th- REE bearing minerals, in radioactive pegmatite in Um swassi-dara area, north Eastern Desert, Egypt. Jordan.At. Energy Comm. 1, 197–209.

Ali, M.A., 2001. Geology, Petrology and Radioactivity of Gabal El-Sibai Area, Central Eastern Desert, Egypt. Ph.D. Thesis. Cairo University 300pp.

Ali, M.A., El-Sawey, E.H., Sadek, A.A., 2008. Mineralogy and radioactivity of the zoned pegmatite bodies, gabal ateila granite, central Eastern Desert, Egypt. Sci.J. Fac. Sci. XXII, 129–145 Minufia University.

Asran, A.M.H., El Mansi, M.M., Ibrahim, M.E., Abdel Ghani, I.M., 2013. Pegmatites of gabal El Urf, central Eastern Desert, Egypt. In: The Seventh International Conference of the Geology of Africa, P-P IV-1 – IV-22 (Nov. 2013), Assuit, Egypt.

Bau, M., 1996. Controls on the fractionation of isovalent trace elements in magmatic and aqueous system; evidence from Y/Ho, Zr/Hf and lanthanide tetrad effect. Contrib. Mineral. Petrol. 123, 323–333.

Bau, M., 1997. The lanthanide tetrad effect in highly evolved felsic igneous rocks-A reply to the comment by Y. Pan. Contrib. Mineral. Petrol. 128, 409–412.

Boyle, R.W., 1982. Geochemical Prospecting for Thorium and Uranium Deposits. Elsevier Publication Company, Amsterdam 498pp.

Boynton, W.V., 1984. Geochemistry of the rare earth elements: meteorite studies. In: Henderson, P. (Ed.), Rare Earth Element Geochemistry. Elsevier, Amsterdam, pp. 63–114.

Caironi, V., Colombo, A., Tunesi, A., Gritti, C., 2000. Chemical variations of zircon compared with morphological evolution during magmatic crystallization: an example from the Valle del Cervo Pluton (Western Alps). Eur. J. Mineral. 12, 779–794.

Cambon, A.R., 1994. Uranium deposits in granitic rocks. In: Notes on the National Training Course on Uranium Geology and Exploration. Organized by International Atomic Energy Agency and Nuclear Material Authority, pp. 8–20.

Cerny, P., 1990. Distribution, affiliation and derivation of rare-element granite pegmatites in Canadian Shield. Geol. Rundsch. 79, 183–226.

Černý, P., 1991. Rare-element granitic pegmatites. 1. Anatomy and internal evolution of pegmatite deposits. Geosci. Can. 18, 49–67.

Černý, P., Burt, D.M., 1984. Paragenesis, and geochemical evolution of micas in granitic pegmatites. In: In: Bailey, S.W. (Ed.), Micas: Mineralogical Society of America, Reviews in Mineralogy, vol. 13. pp. 257–297.

Černý, P., Ercit, T.S., 2005. The classification of granitic pegmatites revisited. Can. Mineral. 43, 2005–2026.

Černý, P., Goad, B.E., Hawthorne, F.C., Chapman, R., 1986. Fractionation trends of the Nb and Ta-bearing oxide minerals in the Greer Lake pegmatitic granite and its pegmatite aureole, southeastern Manitoba. Am. Mineral. 71, 501–517.

Černý, P., London, D., Novak, M., 2012. Granitic pegmatites as reflections of their sources. Elements 8, 289–294.

China National Nuclear Corporation (CNNC), 1993. Research Achievement from Bureau of Geology‖. Internal report, China, 122pp.

Clark, S.P., Petrman, Z.E., Heier, K.S., 1966. Abundance of uranium, thorium and potassium. In: In: Clark Jr.S.P. (Ed.), Handbook of Physical Constraints, vol. 97. Geological Society of American Bulletin, pp. 521–541 Section 24.

Cullers, R.L., Graf, l., 1984. Rare Earth elements in igneous rocks of the continental crust: intermediate and silicic rocks are petrogenesis. In: In: Henderson, P. (Ed.), Rare Earth Elements Geochemistry, vol. 2. Elsevier Publication Company, Amsterdam, pp. 275–316.

Darenely, A.G., Ford, K.L., 1989. Regional airborne gamma-ray survey; a review. In: Proceedings of 3rd International Conference of Geophysical and Geochemical Exploration for Minerals and Ground Water l.3. Geological Survey, Ontario, pp. 229–240.

Dawoud, M.I., Saleh, G.M., Shahin, H.A., Khaleal, F.M., Emad, B.M., 2018. Younger granites and associated pegmatites of gabal El Fereyid – Wadi rahaba area, south Eastern Desert, Egypt: geological and geochemical characteristics. Isaac Scientific Publishing. Geosci. Res. 3 (4), 29–50.

El Amawy, M.A., 1991. Structure and tectonic development of Wadi beitan, Wadi rahaba area, south Eastern Desert, Egypt. In: 9th Symposium on Precambrian Development. National Committee on Geological Science, Cairo, Egypt, P9.

El Aassy, I.E., Shazly, A.G., Hussein, H.A., Heikal, M.T.S., El Gaby, M.M., 1997. Pegmatites of nubeiba-dahab area, west gulf of aqaba, sinai, Egypt: field aspcts, mineralogy, geochemistry and radioactivity. In: The 3rd Conf. On Geochem., Spe., 3-4, 1997, Alex., Egypt.

El Baraga, M.H., 1992. Geological, Mineralogical and Geochemical Studies of the Precambrian Rocks Around Wadi Rahaba, South Eastern Desert, Egypt. PhD Geology. Faculty of Science, Tanta University, Egypt 278pp.

El Eraqi, M.A.F.M., 1990. Geophysical Study on the Area between Latitudes 23 00-25 N and Longitudes 33 30-35 30 E, Southeastern Desert, Egypt. PhD Geophysics. Faculty of Science, Zagazig University, Egypt 289pp.

Gordiyenko, V.V., 1971. Concentrations of Li, Rb, and Cs in potash feldspar and muscovite as criteria for assessingthe rare-metal mineralization in granite pegmatites. Int. Geol. Rev. 13, 134–142.

Heikal, M.Th.S., Moharem, A.F., El Nashar, E.R., 2001. Petrogenesis and radioactive inspection of Li-mica pegmatites at Wadi Zareib, central Eastern Desert, Egypt. In: The Second International Conference on the Geology of Africa, Assiut, Oct. 2001, vol. II. pp. 227–305.

Heikal, M.Th.S., Abedel Monsef, M., El Mansi, M., Gomaa, S.R., Top, G., 2018. Natural radionuclides levels and their geochemical characteristics of Abu dabbab albite granite mining area, central nubian shield of Egypt. J. Environ. Hazards 1, 1–14.

Heikal, M.Th.S., Top, G., 2018. Assessment of radioactivity levels and potential radiation health hazards of Madsus granites and associated dikes nearby and around Ruwisat village, South Sinai, Egypt. J. Afr. Earth Sci. 146, 191–208.

Heikal, M.Th.S., Khedr, M.Z., Abd El Monsef, M., Gomaa, S.R., 2019. Petrogenesis and geodynamic evolution of neoproterozoic Abu dabbab albite granite, central Eastern Desert of Egypt: petrological and geochemical constraints. J. Afr. Earth Sci. 158.

Hermann, A.G., 1970. Yttrium and lanthanides. In: Wedepohl, K.H. (Ed.), Handbook of Geochemistry. Springer, New York, pp. 39–57.

Ibrahim, M.E., Saleh, G.M., Abd El-Naby, H.H., 2001. Uranium mineralization in the two-mica granite of gabal ribdab, south Eastern Desert, Egypt. Journal of Applied Radiation and Isotopes 55/6, 123–134.

Ibrahim, M.E., Shalaby, M.H., Ammar, S.E., 1997. Preliminary studies on some uranium and thorium bearing pegmatites at G. Abu Dob, Central Eastern Desert, Egypt. Proc.Egypt.Acad. Sci. 47, 173–188.

Irber, W., 1999. The lanthanide tetrad effect and its correlation with K/Rb, Eu/Eu*, Sr/Eu, Y/Ho and Zr/Hf of evolving peraluminous granite suites. Geochem. Cosmochim. Acta 63 (3), 489–508.

Jahn, B., Wu, F., Capdevila, R., Martineau, F., Zhao, Z., Wang, Y., 2001. Highly evolved juvenile granites with tetrad REE patterns: the Woduhe and Baerzhe granites from the Great Xing'an Mountains in NE China. Lithos 59, 171–198.

Masuda, A., Kawakami, O., Dohmoto, Y., Takenaka, T., 1987. Lanthanide tetrad effects in nature: two mutually opposite types, W and M. Geochem. J. 21, 119–124.

Mehnert, K.R., Busch, W., 1981. The Ba content of K-feldspar megacrysts in granites. Neus Jahrbuch Mineralogie Abhandlung 140, 221–252.

Mohamed, F.H., Hassanen, M.A., Shalaby, M.H., 1994. Geochemistry of Wadi Hawashia granite complex, northern Egyptian shield. J. Afr. Earth Sci. 19, 61–74.

Nossair, L.M., 1987. Structural and Radiometric Studies of Gebel Gharib Area, North Eastern Desert, Egypt. Ph.D. Thesis. Faculty of Science, Alexandria University 182pp.

Omar, S.A., 1995. Geological and Geochemical Features of the Radioactive Occurrences South G. Um Anab Granitic Masses, Eastern Desert, Egypt. M.Sc. Thesis. Cairo University 164pp.

Owen, M.R., 1987. Hafnium content of detrital zircons, a new tool for provenance study. J. Sediment. Res. 57, 824–830.

Ragab, A.A., 2011. Geochemistry and radioactivity of mineralized pegmatite from Abu Rusheid area, south Eastern Desert, Egypt. JAKU: Earth Sci. 22 (2), 99–130.

Raslan, M.F., Ali, M.A., 2011. Mineralogy and mineral chemistry of rare-metal pegmatites at Abu Rusheid granitic gneisses, South Eastern Desert, Egypt. Geologija 54/2, 205–222.

Raslan, M.F., El Shall, H.E., Omar, S.A., Daher, A.M., 2010. Mineralogy of polymetallic mineralized pegmatite of ras baroud granite, central Eastern Desert, Egypt. J. Mineral. Petrol. Sci. 105 (3), 123–134.

Rogers, J.J.W., Adams, J.A.S., 1969. Uranium and thorium. In: In: Wedepohl, K.H. (Ed.), Handbook of Geochemistry, vol. 4 Springer Venleg, New York 92-B-1 to92-C-10.

Saleh, G.M., Dawoud, M.I., Shahin, H.A., Khaleal, F.M., Emad, B.M., 2018. Gabal El Fereyid - Wadi rahaba area, south Eastern Desert, Egypt: mineralization and spectrometric prospecting. Int. J. Min. Sci. 4 (2), 1–15.

Salem, I.A., Heikal, M.Th.S., Ashmawy, M.H., 1998. Rod Ashab mica-bearing pegmatite,

Eastern Desert, Egypt: a model for the derivation of anatexis. In: Proceedings of 1st Symposium "Geology of the Pre-cretaceous and Development in Egypt". Zagazig, pp. 1–26.
Sayyah, T.A., Assaf, H.S., Abdel Kader, Z.M., Mahdy, M.A., Omar, S.A., 1993. New Nb-Ta occurrence in gebel ras baroud, central Eastern Desert, Egypt. Egyptian Mineralogist 5, 41–55.
Shalaby, M.H., 1985. Geology and Radioactivity of W. Dara Area, North Eastern Desert, Egypt. Ph.D. Thesis. Faculty of Science, Alexandria University 165pp.
Soliman, M.M., Atawia, M.Y., Ali, M.M., Abdel-Karim, A.M., 1985a. Petrography and geochemistry of some younger granite masses in the south Eastern Desert of Egypt. Bulletin of Faculty of Science, Zagazig University 7, 90–129.
Soliman, M.M., Atawia, M.Y., Ali, M.M., Abdel-Karim, A.M., 1985b. The geochemistry and petrogenesis of the Precambrian gabbro-tonalite complex of Wadi El-Rahaba area, south Eastern Desert, Egypt. Bulletin of Faculty of Science, Zagazig University 7, 130–155.
Stuckless, J.S., Bunker, C.M., Bush, C.A., Doering, W.P., Scott, J.I.I., 1977. Geochemical and petrologic studies of a uraniferous granites of the Granite Mountains, Wyoming. U.S. Geol .Surv.J.Res. 5, 61–81.
Sun, S.S., McDonough, W.F., 1989. Chemical and isotopic systematic of oceanic basalts: implications for mantle composition and processes. In: Saunders, A.D., Norry, M.J. (Eds.), Magmatism in the Ocean Basins.
Sweetapple, M.T., 2000. Characteristics of Sn-Ta-Be-Li-Industrial Mineral Deposits of the Archaean Pilbara Craton. Australian Geological Survey Organization, Western Australia. Canberra AGSO Record 2000/44: 54.
Thomas, R., Webster, J.D., 2000. Characteristics of berlinite from the ehrenfriedersdorf pegmatite, erzgebirge, Germany. Eur. J. Mineral. 281, 124–136.
Trueman, D.L., Černý, P., 1982. Exploration for rare element granitic pegmatites in science and industry: mineralogical Association of Canada. Short Course Handb. 8, 463–493.
Uher, P., Černý, P., 1998. Zircon in hercynian granitic pegmatites of the western Carpathians, Slovakia. Geol. Carpathica 49, 261–270.
Walker, R.J., 1984. The Origin of the Tin Mountain Pegmatite, Black Hills, South Dakota. Ph.D. thesis. State University of New York at Stony Brook 170pp.
Wang, X., Griffin, W.L., Chen, J., 2010. Hf Contents and Zr/Hf ratios in granitic zircons. Geochem. J. 44, 65–72.
Worral, F., Pearson, D.G., 2001. Water-rock interaction in an acidic mine discharge as indicated by rare earth element patterns. Geochem. Cosmochim. Acta 65, 3027–3040.